

 Open access • Journal Article • DOI:10.1109/23.603798

## A linear low power remote preamplifier for the ATLAS liquid argon EM calorimeter

— [Source link](#) 





R. L. Chase, S. Rescia

**Published on:** 02 Nov 1996 - IEEE Nuclear Science Symposium

**Topics:** Preamplifier, Amplifier, Noise (electronics), Input impedance and Electric power transmission

Related papers:

- [Transmission line connections between detector and front end electronics in liquid argon calorimetry](#)
- [Physics potential and experimental challenges of the LHC luminosity upgrade](#)
- [Improvement of the gain of MOS amplifiers](#)
- [Feedforward compensation techniques for high-frequency CMOS amplifiers](#)
- [MAROC: Multi-Anode ReadOut Chip for MaPMTs](#)

Share this paper:    

View more about this paper here: <https://typeset.io/papers/a-linear-low-power-remote-preamplifier-for-the-atlas-liquid-1mah0j9v5h>

# A Linear Low Power Remote Preamplifier for the Atlas Liquid Argon EM Calorimeter<sup>1</sup>

R. L. Chase<sup>1</sup> and S. Rescia<sup>2</sup>

<sup>1</sup>Laboratoire de l'Accélérateur Linéaire 91405 Orsay, France

<sup>2</sup>Brookhaven National Laboratory Upton, NY 11973-5000

## Abstract

In a previous paper [1], it was shown that, for shaping times of the order of the transmission line delay, a remote, external preamplifier could perform as well as one connected directly to a liquid argon calorimeter. Here we describe an improved circuit configuration where, by attributing the functions of low noise and high dynamic range to two different transistors, the linearity can be improved and the noise can be decreased while reducing the power dissipation by a factor of three (to about 50 mW). The gain (i.e., the transresistance) and the input impedance can be chosen independently without changing the power supply voltages and power dissipation.

## I. INTRODUCTION

In order to maximize the signal-to-noise ratio, it has been conventional wisdom to use very short connections between radiation detectors and their preamplifiers so as to minimize the total input capacitance. In a previous paper [1], it was shown that, under certain circumstances, as good, or even slightly better signal-to-noise ratios could be achieved with a transmission line connecting the detector to the preamplifier. This can be true, provided that:

1. pile-up considerations impose a shaping time that is of the order of, or shorter than the transmission line propagation time;
2. the reactance of the detector capacitance is of the order of the transmission line characteristic impedance at the center frequency of the shaping filter;
3. the input time constant, determined by the detector capacitance and the transmission line impedance is not long compared to the shaping time.

To prevent multiple reflections, the transmission line must be terminated in its characteristic impedance at the preamplifier. A physical resistance should not be used as it would normally be the dominant noise source. Conventionally [2], an "electronically cooled" termination is used, created by an operational amplifier with capacitive feedback, whose input resistance is, approximately:

$$\frac{C_p}{g_m \cdot C_f} \quad (1)$$

<sup>1</sup> This research was supported by the U. S. Department of Energy: Contract No. DE-AC02-76CH00016.

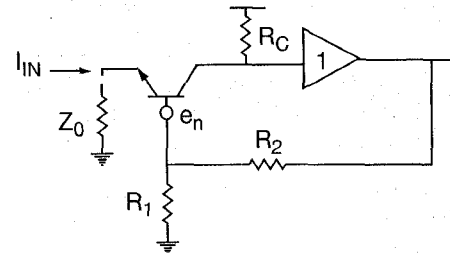


Figure 1: Circuit schematic of the line terminating preamplifier described in [1]. It has a power dissipation of about 140 mW.

where  $C_p$  is the dominant pole capacitance of the operational amplifier,  $C_f$  is the feedback capacitance and  $g_m$  is the input element transconductance.

This solution works well, provided that the input signal amplitude is not large enough to produce significant changes in the input amplifier transconductance. In the case of liquid argon calorimeters on high energy accelerators, this may not be the case, since signal currents may approach 10 mA or more and the corresponding voltage signal at the preamplifier input can substantially change the transconductance.

The preamplifier configuration presented in [1], and reproduced here as figure 1, is better adapted to these high dynamic range applications. Here, the equivalent "cooled" input resistance is:

$$\frac{1}{g_m} + R_c \cdot \frac{R_1}{R_1 + R_2} \quad (2)$$

where  $R_c$  is the collector load resistance,  $R_1$  and  $R_2$  are the feedback resistances and  $g_m$  is the transconductance of the input transistor. The input transistor current is chosen to be high (about 4 mA) for low noise and to render the first term in expression 2, which varies with signal amplitude, small compared to the second term.

Although this circuit works relatively well, it has a few drawbacks:

1. in the case of low impedance transmission lines (25  $\Omega$ ), a very large input current would be necessary to make the first term in expression 2 small enough to achieve 1% non-linearity;
2. a high power supply voltage is required to prevent the input transistors from saturating with a large signal current,

particularly if the dc current is also large. This leads to high power dissipation, limits the choice of input transistors and excludes the use of most integration technologies;

3. great care is required to prevent the input stage from oscillating at a high frequency ( $\sim 1$  GHz) since transistors with high  $f_t$  are required for a low value of the base spreading resistance  $r_{bb'}$ , and stopper resistors would add too much noise.

## II. HIGH LINEARITY, REDUCED POWER LINE TERMINATING PREAMPLIFIER

To circumvent these drawbacks, we propose a different circuit configuration which, by assigning the functions of low noise and large dynamic range to different transistors, insures a better linearity while also allowing a reduction of the power dissipation.

### A. The Inner Feedback Loop

To improve the integral non-linearity of the circuit, it is necessary to stabilize the input impedance against signal-induced changes. This can be achieved by reducing the first term of expression 2 with respect to the second.

The circuit of figure 2 achieves such a goal. The transistor

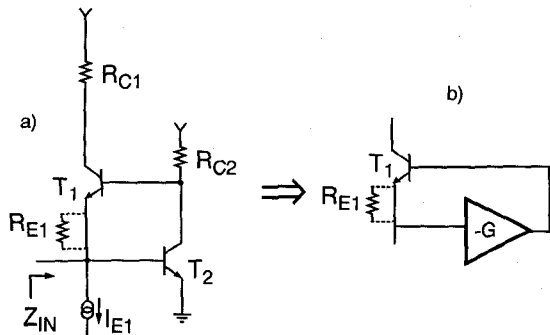


Figure 2: Feedback loop used to reduce the input impedance component dependent on the signal. The transistor  $T_2$  and its collector resistor  $R_{C2}$  amplify the base-emitter voltage of the input transistor  $T_1$ . Hence,  $T_1$  input impedance is reduced by the loop gain  $G$ . The resistor,  $R_{E1}$  ( $\sim 100 \Omega$ ) in series with the emitter is necessary to stabilize the loop. The resulting input impedance is:  $Z_{in} = (1/g_{m1} + R_{E1})/G$ .

$T_2$  and its collector resistor  $R_{C2}$  amplify the base emitter voltage of  $T_1$  (see fig. 2b). Hence, the input impedance of  $T_1$  is reduced by the loop gain  $G$ . It is necessary to add a resistor,  $R_{E1}$  ( $\sim 100 \Omega$ ) in series with the emitter of  $T_1$  to make the loop stable. The resulting input impedance is:

$$Z_{in} = \frac{1/g_{m1} + R_{E1}}{G} \quad (3)$$

### B. The External Loop

Another feedback loop (figure 3) is needed to achieve the

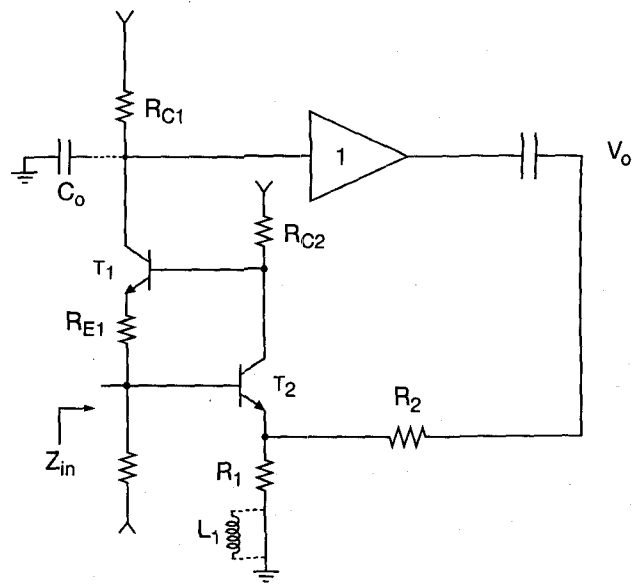


Figure 3: Simplified circuit diagram of the line terminating preamplifier. The external feedback loop increases the input impedance of the  $T_1 - T_2$  inner loop to the value:  $Z_{in} = (1/g_{m1} + R_{E1})/G + R_{C1} \times R_1 / (R_1 + R_2)$ . The addition of the inductor  $L_1$  in series with  $R_1$  achieves a pole-zero cancellation of the pole  $R_{C1} \times C_0$ , thus extending the bandwidth.

desired input impedance. A straightforward calculation (see Appendix 1) shows that the input impedance can be approximated as:

$$Z_{in} = \frac{1/g_{m1} + R_{E1}}{G} + \frac{R_{C1}}{1 + R_2/R_1} \quad (4)$$

where:

$$G = \frac{1}{1/g_{m2} + R_1} \times R_{C2} \quad (5)$$

is the loop gain of the inner loop, taking into account the emitter degeneration introduced by  $R_1$ .

### C. Noise Equivalent Circuit

It is easy to see that both the noise generated by  $T_1$  and by  $R_{E1}$ , appear attenuated by a factor  $G$  with respect to any noise source which can be represented by a voltage noise generator in series with the base of  $T_2$ . Appendix 2 shows that such a generator can be moved outside of the loop. The equivalent series noise generator is dominated by the collector shot noise of  $T_2$ , its base spreading resistance,  $r_{bb'}$ , and the noise of  $R_1$  ( $R_2 \gg R_1$ ). Figure 4 shows all the dominant noise sources of this circuit configuration.

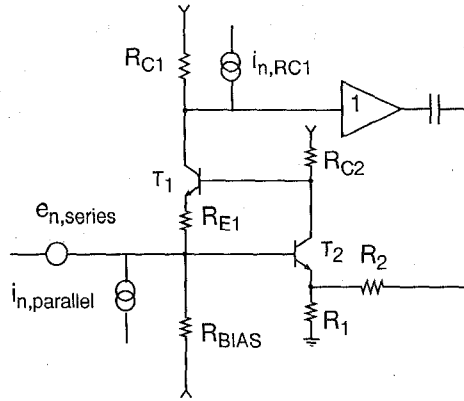


Figure 4: Equivalent noise sources for the line terminating preamplifier. The values for the noise generators are:

$$e_{n,series}^2 = 4K_B T \left( \frac{1}{2g_{m2}} + r_{bb'2} + R_1 \right)$$

$$i_{n,parallel}^2 = \frac{4K_B T}{R_{BIAS}} + 2q(I_{B1} + I_{B2})$$

$$i_{n,RC1}^2 = \frac{4K_B T}{R_{C1}}$$

where  $K_B$  is the Boltzmann constant,  $T$  the temperature in degrees Kelvin,  $g_{m2}$  and  $r_{bb'2}$  the transconductance and the base spreading resistance of the  $T_2$  input transistor pair,  $I_{B1}$ ,  $I_{B2}$  the base currents of  $T_1$  and  $T_2$  and  $R_2 \gg R_1$ .

#### D. Advantages of the New Configuration

Figure 5 shows the full circuit diagram. The unity gain buffer is a White follower as in the previous circuit. A current source transistor has been added for biasing the White follower. This allows various values of the resistor  $R_{C1}$  to be chosen to adapt to different dynamic range requirements in various parts of the detector, without changing the operating conditions. The input resistance is made to match the line impedance by appropriate choice of the feedback divider ratio, for each value of  $R_{C1}$ .

The major advantage of the proposed configuration is that the functions of providing low noise and high dynamic range are separated and assigned to different transistors. The pair of input transistors ( $T_2$  and  $T_2'$ , connected in parallel to reduce the base spreading resistance) operate at high current ( $\sim 7$  mA) for low noise, but from a low supply voltage (3 V) and, therefore, has modest dissipation.  $T_1$ , which absorbs the input current, has a low dc bias current ( $\sim 1$  mA). Even with high collector voltage its dissipation is moderately low.

The loop gain of the input stage is about 33. Variations of the input impedance with signal current (due both to a change in the  $1/g_{m1}$  term and the gain  $G$  in expression 4) are now reduced to about  $\Delta Z_{in} = 0.6 \Omega$  or 2.4% for  $Z_{in} = 25 \Omega$  and an input current of 5 mA. In the previous configuration, the resistance change with signal was about  $4.5 \Omega$  or 18%.

As in the previous configuration, a small inductor has been added in series with  $R_1$  to decrease the mismatch at high frequency due to the pole at the collector of  $T_1$ ,  $\tau_0 = R_{C1} \times C_0$ , where  $C_0$  is the total capacitance on that node. The input impedance  $Z_{in}$  becomes:

$$Z_{in} = \frac{1}{G} \left( \frac{1}{g_{m1}} + R_{E1} \right) + \frac{R_1 + sL_1}{R_1 + R_2 + sL_1} \times \frac{R_{C1}}{1 + sR_{C1}C_0} \quad (6)$$

By equating the time constant of the pole  $\tau_0$  and the zero  $\tau_z = L_1/R_1$ , it follows that:

$$Z_{in} = \frac{1}{G} \left( \frac{1}{g_{m1}} + R_{E1} \right) + \frac{R_1}{R_1 + R_2} \times \frac{R_{C1}}{1 + sR_{C1}C_0 \times \frac{R_1}{R_1 + R_2}} \quad (7)$$

and the bandwidth is extended by a factor  $(R_1 + R_2)/R_1$ .

A slight noise improvement, with respect to the previous circuit has been measured. This is partly due to the fact that the bias resistor defining the current in  $T_1$  is now larger ( $4 \text{ k}\Omega$ , because of the lower DC current) and also to the lower series noise achieved by increasing the bias current of the input transistor pair. Further noise reduction would be possible by monolithic integration of the circuit. Fast, low noise bipolar processes which have a  $V_{CEO}$  voltage typically less than 5 or 6 V are now usable. The size of the input transistor could, therefore, be increased, thus decreasing the net value of  $r_{bb'}$ . To benefit from such a reduction, the value of  $R_1$  must also be decreased.

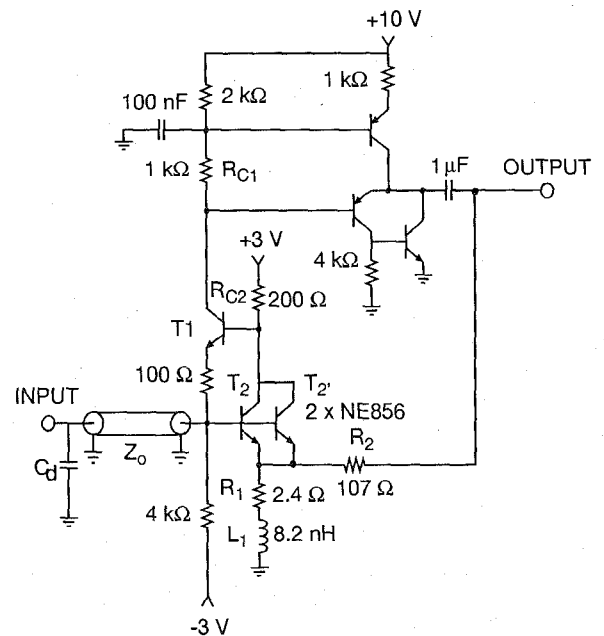


Figure 5: Full schematic of the line terminating preamplifier for  $Z_{in} = 25 \Omega$  and a maximum input current of 5 mA. For an input impedance of  $Z_{in} = 50 \Omega$  and a maximum input current of 1 mA the values are:  $R_{C1} = 3.3 \text{ k}\Omega$ ,  $R_2 = 158 \Omega$ ,  $L_1 = 18 \text{ nH}$ . Power supply filtering and discharge protection network not shown.

### III. EXPERIMENTAL RESULTS

Figure 6 a,b show the preamplifier and shaper response to the liquid argon signal (a triangular current pulse with a duration  $t_d = 400$  ns and initial current  $I_0 = 1$  mA) of the preamplifier with  $Z_{in} = 50 \Omega$ . The preamplifier rise time (10% to 90%) is about 45 ns, dominated by the input time constant  $\tau_{in} = C_D \times Z_0 = 400$  pF  $\times$   $50 \Omega = 20$  ns. The shaper is a CR-RC<sup>2</sup> filter with a time constant  $\tau_{SH} \sim 20$  ns. The liquid argon signal peaking time is about 40 ns (5% to 100%).

Linearity problems are more severe for the  $Z_{in} = 25 \Omega$  preamplifier, particularly when it is used over a wide dynamic range, since the change of the first term in expression 4 is proportionally larger.

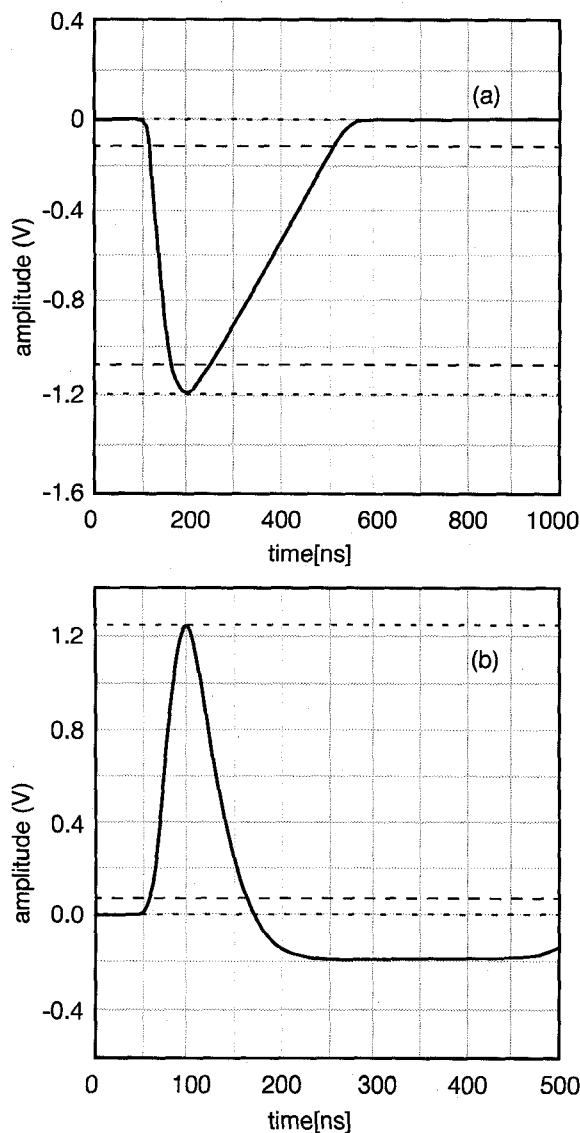


Figure 6: Preamplifier response (a) and shaper response (b) for a LAr type triangular current pulse of duration  $t_d = 400$  ns. The other parameters are:  $I_0 = 1$  mA,  $C_d = 400$  pF,  $Z_{in} = 50 \Omega$ ,  $L = 3$  m miniature Kapton insulated coax at  $T = 77$  K. The 10%-90% rise time is about 45 ns. The shaper response is for a CR-RC<sup>2</sup> filter with a 40 ns peaking time (5%-100%) for a LAr excitation.

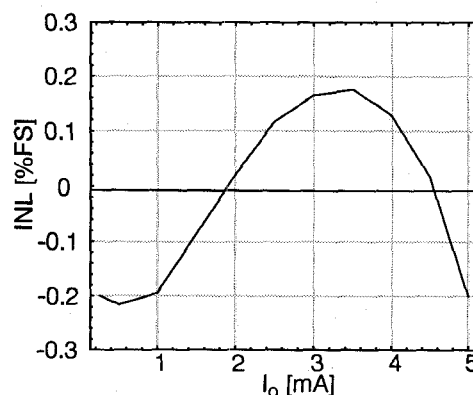


Figure 7: Integral non-linearity of the line terminating preamplifier over the full dynamic range is  $\pm 0.2\%$ .

Figure 7 shows the integral non-linearity plot for the  $Z_{in} = 25 \Omega$  preamplifier. Over a 5 mA dynamic range, it was found to be  $\pm 0.2\%$ . A number of units have been fabricated and tested. They show consistent performance, summarized in Table 1.

Table 1.  
Preamplifier Test Results

|                                     | $Z_{in} = 50 \Omega$ | $Z_{in} = 25 \Omega$ |
|-------------------------------------|----------------------|----------------------|
| Number of unit tested               | 11                   | 32                   |
| $C_{det}$                           | 400 pF               | 2200 pF              |
| Power Dissipation                   | 47 mW                | 47 mW                |
| Line Length                         | 3 m                  | 3 m                  |
| $I_{o,max}$                         | 1 mA                 | 5 mA                 |
| $R_{C1}$                            | 3300 $\Omega$        | 1000 $\Omega$        |
| $R_2$                               | 158 $\Omega$         | 107 $\Omega$         |
| Integral Linearity                  | $\pm 0.2\%$          | $\pm 0.2\%$          |
| ENI (average) @ $t_{pk,tr} = 40$ ns | 66 nA                | 275 nA               |
| Gain Tolerance                      | $\pm 2\%$            | $\pm 2\%$            |
| Peaking Time Tol.                   | $\pm 1$ ns           | $\pm 1$ ns           |
| Noise Tolerance                     | $\pm 5\%$            | $\pm 5\%$            |

### IV. ACKNOWLEDGMENTS

We wish to thank Veljko Radeka for his support and many stimulating discussions. We also want to thank Mauro Citterio for his help in the characterization and Frank Densing for his expert layout of the circuit.

## Appendix 1: Derivation of the Input Impedance

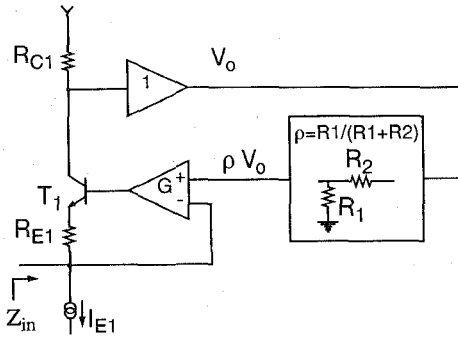


Figure 8: Equivalent representation of the circuit of figure 3 for the calculation of the input impedance  $Z_{in}$  presented at the input.

Figure 8 shows an equivalent representation of the circuit of figure 3. The triangle represents a “current mode feedback” gain block whose high and low impedance inputs are respectively the base and the emitter of  $T_2$ .

A straightforward calculation allows us to derive the expression for  $Z_{in}$  (which assumes an infinite input impedance for  $T_1$ , or  $\beta_1 \rightarrow \infty$ ):

$$Z_{in} = \frac{1/g_{m1} + R_{E1}}{G + 1} + \frac{G}{G + 1} \times \frac{R_{C1}}{1 + R_2/R_1} \quad (8)$$

for  $G \gg 1$ , it can be simplified:

$$Z_{in} = \frac{1/g_{m1} + R_{E1}}{G} + \frac{R_{C1}}{1 + R_2/R_1} \quad (9)$$

where

$$G \cong \frac{1}{1/g_{m2} + R_1} \times R_{C2} \quad (10)$$

is the loop gain of the inner feedback loop.

## Appendix 2: Derivation of the Equivalent Series Noise Generator

Let us consider the simplified inner feedback loop of figure 9. We want to compute the equivalent series noise generator,  $e_{n,eq}$  of the noise generator in series with the noise of  $T_2$ ,  $e_{n2}$  by computing the equivalent Thevenin generator of  $e_{n2}$ . To this extent, we need to compute the unloaded voltage swing of the emitter of  $T_1$  due to  $e_{n2}$ . The equivalent circuit is shown in figure 10.

We have:

$$\begin{cases} V_{be1} = V_{b1} - V_{e1} = -(G + 1)V_{e1} + e_{n2} \cdot G \\ g_{m1}V_{be1} + V_{be1}/r_{b1} = 0 \Rightarrow V_{be1} = 0 \end{cases} \quad (11)$$

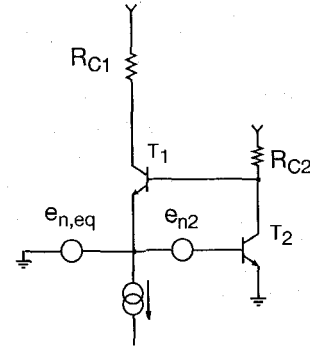


Figure 9: Simplified circuit for the calculation of the equivalent series noise voltage generator  $e_{n,eq}$  of the generator  $e_{n,2}$ .

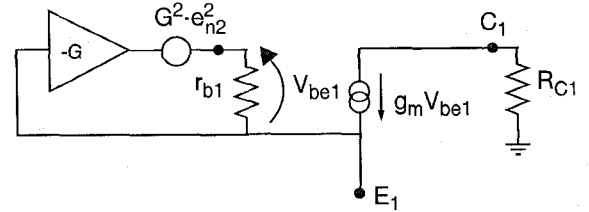


Figure 10: Equivalent representation of the circuit of figure 9.

which yields:

$$V_{e1} = e_{n2} \cdot \frac{G}{G + 1} \cong e_{n2} \quad (12)$$

for  $G \gg 1$ .

Closing the external feedback loop will add the noise of the feedback elements ( $R_1$ ,  $R_2$  and the unity gain buffer), but will not change the noise generator. Including the external feedback noise sources, we have:

$$e_{n,eq}^2 = e_{n2}^2 = 4K_B T \left( \frac{1}{2g_{m2}} + r_{bb'2} + R_1 \right) \quad (13)$$

assuming  $R_1 \gg R_2$ .

As explained in section II: C, the noise of the resistor  $R_{E1}$  and the collector shot noise of  $T_1$  appear divided by the loop gain  $G$  (~33) and are, therefore, negligible.

## V. REFERENCES

- [1] R.L. Chase, C. de La Taille, S. Rescia and N. Seguin, “Transmission Line Connections Between Detector and Front End Electronics in Liquid Argon Calorimetry”, *Nucl. Instrum. & Meth.*, A330, pp. 228-242, 1993.
- [2] V. Radeka, “Signal, Noise and Resolution in Position Sensitive Detectors”, *IEEE Trans. Nucl. Sci.*, NS-21 No. 1, pp. 51-64, Feb. 1974.